IEEE Access
Multidisciplinary | Rapid Review | Open Access Journal

Received April 16, 2019, accepted May 11, 2019, date of publication May 20, 2019, date of current version May 31, 2019.

Digital Object Identifier 10.1109/ACCESS.2019.2917724

Recursive Observation Evidence Fusion Method for Acoustic Resonance-Based Level Detection

XIAOBIN XU, DANFENG FANG, GUO LI, PENG CHEN, XIAOJIAN XU, AND JIANNING LI
School of Automation, Hangzhou Dianzi University, Hangzhou 310018, China

Corresponding author: Xiaobin Xu (xuxiaobin1980@163.com)

This work was supported in part by the NSFC-Zhejiang Joint Fund for the Integration of Industrialization and Informatization under Grant U1709215, in part by the NSFC under Grant 61433001 and Grant 61733009, and in part by the Zhejiang Province Key R&D Projects under Grant 2019C03104 and Grant 2018C01031 of Hangzhou Yan Shi Technology Co., Ltd.

ABSTRACT Acoustic resonance-based level measurement principle needs to extract a sequence of resonance frequencies (RFs) from the synthesis wave and then calculate level height via this RF sequence. However, in practice, the uncertain disturbances in the measurement environment usually lead to the signal distortion of the collected synthesis wave. In this case, some RF points in the sequence are inevitably missed which causes the nonnegligible calculation error. Hence, based on the Dempster-Shafer evidence theory (DST), this paper presents a recursive evidence fusion method to combine multiple RF sequences in a row. It provides a natural way to supplement the missed RF points and also significantly improve the measurement accuracy even if the observed RF sequences are all intact. That is to say, regardless of the missing case or intact case, the proposed fusion method always has high performance. Finally, the comparative experiments of level detection show the level gauge using this method is robust for the sequence with the missing RF points and can further provide higher measurement accuracy than the single RF sequence-based and digital filtering-based level detection methods.

INDEX TERMS Level detection, acoustic resonance, DS evidence theory (DST), random-fuzzy variable (RFV), alarm monitoring.

I. INTRODUCTION

Sound reflection-based liquid level measurement is a kind of widely used method in industry systems including hazardous chemical storage and process, waste water treatment, nuclear reaction, environmental protection, alarm monitoring, safety production, and so on [1], [2]. Generally, the ultrasound reflection principle is adopted to calculate the distance from liquid surface to ultrasound receiver through multiplying the sound velocity by the sound round-trip time. However, when the ultrasound is transmitted to some barriers on the surface, such as foams, residues, and surface ripples, the emerging parasitic reflections will disturb the sound travel path so as to considerably degrade the measurement accuracy [3], [4].

Fortunately, another low-frequency acoustic resonance principle is presented in [5] to avoid the parasitic reflections since the low-frequency sound wave can effectively bypass these barriers (namely, diffraction phenomena) to the liquid surface and then reflect. In detail, a speaker emits sound waves with a uniform change from a frequency f_L to a higher frequency f_H toward the surface, and a microphone receives the synthetic of the transmitted and reflected sound pressure waves. Here, the acoustic resonance will appear, and the first (fundamental) resonance frequency (RF) extracted from the synthesis wave can be used to calculate the height of liquid level. As an alternative to ultrasonic and some other level measurement methods, many researchers pay attention to this novel principle, and make some significant developments and applications. Reference [6] introduced a neural-network classifier to recognize the different operation conditions (residues, foams, deposits) and extracted the corresponding fundamental RF. Reference [7] further studied on a robust miniature acoustical liquid level gauge based on this principle. Reference [8] designed an acoustic resonance device to detect the level of waste water. Reference [9] presented the Unscented Kalman filter to reduce measurement noise of RFs.

Recently, an improved method has been systematically studied in [10], which does not adopt the single fundamental RF but a group of RFs extracted in a given sweep frequency range to calculate level height. Thus, the measured length

The associate editor coordinating the review of this manuscript and approving it for publication was Syed Mohammad Zafaruddin.

is increased from the original 8.6 m to more than 10 m when the medium gas is air, meanwhile the measurement period is reduced from 2 min to 2 s. Because the sequence of RFs can provide more observation information than the single fundamental RF, the improved method has the natural advantage over the classical one in measurement accuracy. In addition, the precondition of ensuring ideal measurement accuracy is that all RF points have to be extracted from the synthesis wave so as to construct an intact RF sequence. However, by analyzing a large number of experiments, it is found that, due to uncertain disturbances in measurement environment or imperfect operation conditions, the collected synthesis wave sometimes tends to be distorted so that some RF points in the sequence are inevitably missed which leads to distinct decrease in measurement accuracy.

In order to deal with the uncertainty of acoustic resonance signals, based on DST [11], this paper presents an evidence-based frequency detection method for supplementing the missed FR points. Firstly, the smoothing filter algorithm proposed in [12] is used to detect the RF sequence from the synthesis wave; secondly, the random-fuzzy variable (RFV) approach is proposed to transform a RF point to a piece of RF evidence; thirdly, the multiple RF evidence sequences acquired in adjacent measurement period are recursively fused by using Dempster's rule so that the missed FR points can be automatically estimated from the fused results. Finally, an experimental gauge is set up by using embedded system, and then the proposed method is tested within a wide range from 0.6 m to 10.8 m showing better performance than the classical methods including the limit range filtering-based method and the original acoustic resonance detector which ignores the missing RF points in sequences.

The rest of the paper is organized as follows: Section II briefly reviews the RF sequence-based level detection principle. Section III introduces the basics of DST and RFV. The recursive observation evidence fusion method is presented in Section IV. Section V analyzes the setting and measuring result of experiments. In Section VI, some concluding remarks are presented.

II. THE LEVEL DETECTION PRINCIPLE VIA THE RF SEQUENCE

The principle is realized by the following level gauge in Fig.1 [10]. Obviously, this gauge has a sample structure consisting of some inexpensive components. Here, the controller gives a command to the speaker to vertically transmit a sweep sound signal y_1 uniformly changing from f_L to f_H toward the surface, nearly meanwhile the reflected wave y_2 is generated on the surface and propagates in the tube. Thus, the microphone can receive their synthesis wave y, as shown in (1)–(3) respectively.

$$y_1 = A\cos 2\pi f(t - \frac{L}{c}) \tag{1}$$

$$y_2 = A\cos 2\pi f(t + \frac{L}{c}) \tag{2}$$

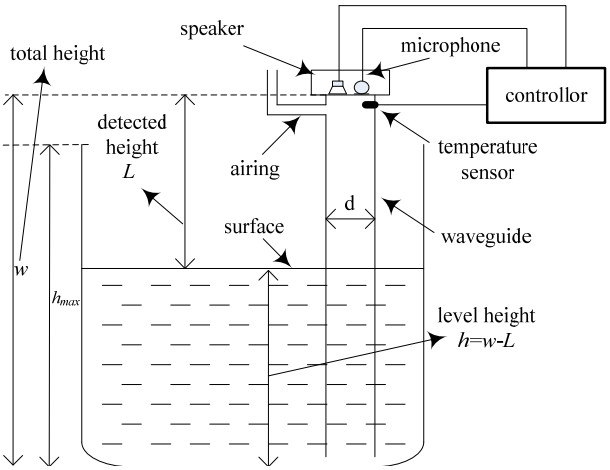

FIGURE 1. Structure of the level gauge.

$$y = 2A\cos\left(2\pi f\frac{L}{c}\right)\cos(2\pi ft) \tag{3}$$

where, A and $f \in [f_L, f_H]$ are the amplitude and frequency respectively, L is the detected height from the top to the surface as marked in Fig.1. c (m/s) and T(° C) are the sound velocity and temperature in air respectively, here $c = 331.4 + 0.6T$. Note that y_1 and y_2 are derived from the sound pressure $A\cos 2\pi ft$ commanded by the controller and collected at the surface. Hence, relative to the original signal $A\cos 2\pi ft$, y_1 and y_2 have the propagation time $-L/c$(earlier) and $+L/c$(later) respectively. More importantly, this propagation time (or the phase shift $2\pi fL/c$) directly relates to the detected height L.

From (3), it can be deduced that the amplitude of synthesis wave will reach to maximum when L is an integral multiple (n) of the half wave length, namely

$$L = n\frac{c}{2f_n} = n\frac{\lambda_n}{2} n = 1, 2, 3, \cdots \tag{4}$$

where, f_n and λ_n are defined as the corresponding resonance frequency and wavelength. Hence, if f_n or λ_n, the mode n,T can be obtained, then L can be calculated. Especially, [5-7] uses the fundamental RF (n =1) to calculate the level height as

$$h = w - L = w - \frac{c}{2f_1} \tag{5}$$

However, if $L \geq 8.28$ m here the medium gas is air, then the fundamental RF will reduce to less than 20Hz which is the lower limit of ordinary microphones. Hence, in order to increase the measuring range, instead of the fundamental RF, [10] proposed to use the RF sequence collected in the synthesis wave y in (3) to calculate L since the lower and upper limits (f_L, f_H) of f can be designed to the values larger than 20Hz, for example $f_L = 1000$ Hz, $f_H = 2000$ Hz. As a result, (4) can be changed as

$$L = \frac{n(i)c}{2f(i)} i = 1, 2, \cdots, M \tag{6}$$

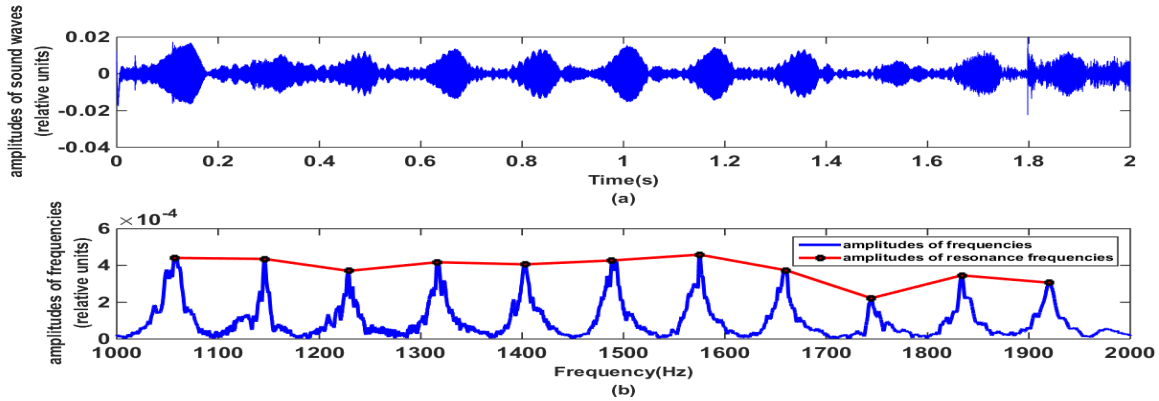

FIGURE 2. The synthesis wave (a) and the intact RF sequence (b) for $L = 2$m.

here $f(i)$ is defined as the i^{th} RF collected in the range $[f_l, f_h]$, $n(i)$ is mode of $f(i)$, M is the number of RFs. Besides $f(i)$, $n(i)$ is calculated by the following equations

$$L = \frac{n(i)c}{2f(i)} = \frac{n(i+1)c}{2f(i+1)} \tag{7}$$

$$\frac{n(i)}{f(i)} = \frac{n(i+1)}{f(i+1)} = \frac{n(i)+1}{f(i+1)} \tag{8}$$

$$n(i)f(i+1) = f(i)n(i) + f(i) \tag{9}$$

thus

$$n(i) = \frac{f(i)}{f(i+1) - f(i)} \tag{10}$$

Although $n(i)$ should be a positive integer in theory, usually it is not like that in practice because $f(i)$ and $f(i+1)$ have observation errors. So the nearest integer value $[n(i)]$ to $n(i)$ is taken and substituted into (6)

$$L = \frac{[n(i)]\,c}{2f(i)} \tag{11}$$

Thus, the level height can be obtained by

$$h = w - \overline{L} \tag{12}$$

where

$$\bar{L} = \frac{\left(\sum_{i=1}^{M-1}\left([n(i)]\,c/2f(i)\right)\right)}{M-1} \tag{13}$$

is the mean of $M-1$ times measurements so as to effectively reduce the errors.

On the other hand, there is a key problem that if certain RF points are not detected then $n(i)$ calculated by (10) will has large deviation such that the exact value of L is hardly obtained by (13). However in real measurement, because of uncertain disturbances in measurement environment or imperfect operation conditions, such unsatisfactory case is unavoidable even though the available smoothing filter is used as given in [12].

For example, for the level gauge shown in Fig.1, when the liquid in the tank is distilled water and the gas in the waveguide is air, the real L is set to 2 m, the frequency of the transmitted sound wave changes from $f_L = 1000$ Hz to $f_H = 2000$ Hz with uniform speed, the time-domain synthesis wave y received by the microphone is shown in Fig.2 (a). Obviously, there are 11 times resonances in 2s or the range [1000Hz, 2000Hz]. In order to extract the RF points from the synthesis wave in noisy environment, Fast Fourier Transform (FFT) and the smoothing filter based on amplitude detection presented in [12] is used to extract 11 RF points as shown in Fig.2 (b). Certainly, this RF sequence with 11 RF points is intact so L can be relatively accurately calculated. On the contrary, Fig.3(a) shows the unsatisfactory case here the 9^{th} resonance wave never comes into being because y is polluted by uncertain noises so that the filter hardly extracts the corresponding RF points from the spectrogram of y in Fig.3(b).

Table 1 and Table 2 list the RF points detected by the filter in [12], L calculated by (13) and the corresponding parameters i and $[n(i)]$ for the intact and incomplete cases respectively. Obviously, the missing of the 9^{th} RF point leads to the ordering errors after $i = 8$ such that the calculated $L = 1.89$ m badly less than the real 2 m. Certainly, in some experiments, the number of the missed RF points in a RF sequence is even more than one. Hence the problem of the missed RF points have to be deal with for preventing the decrease in measurement accuracy. In the following sections, based on DST and random-fuzzy variable (RFV) model, we will present the evidence-based fusion method for combining intact and incomplete RF sequence to automatically supplement the missed FR points.

III. THE BASICS OF DS EVIDENCE THEORY AND RANDOM FUZZY VARIABLE

This section introduces some necessary concepts of the DST and RFV that will be used in the proposed approach. A more detailed explanation and some background information can be found in [11], [13], [14].

A. FOUNDATIONS OF DS EVIDENCE THEORY

The basic framework of the DS theory was proposed by Dempster and Shafer, which defines the basic belief assignment function (BBA), also called evidence, to model

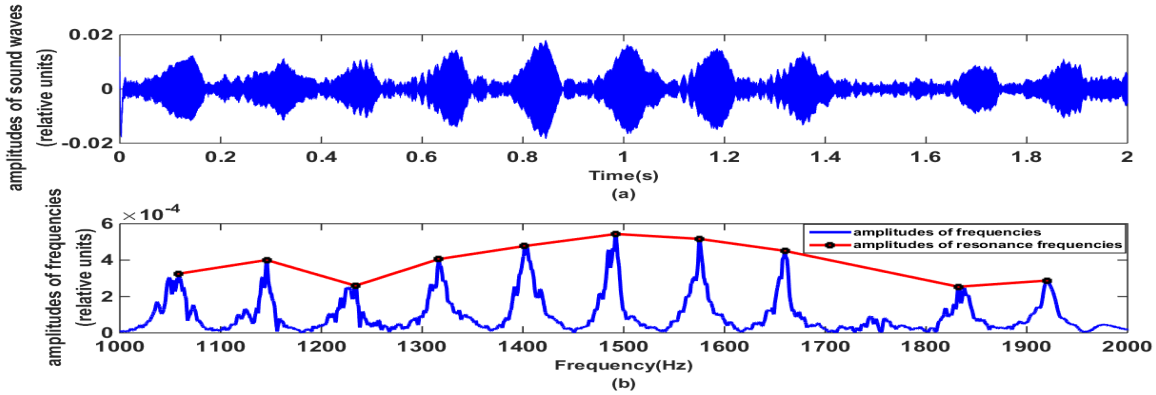

FIGURE 3. The synthesis wave (a) and the incomplete RF sequence (b) for $L = 2$m.

TABLE 1. The intact RF sequence and the calculated L.

i	1	2	3	4	5	6	7	8	9	10	11	T(℃)	L(m)
$[n(i)]$	12	13	14	15	16	17	18	19	20	21	-	27	2.02
RF(Hz)	1057.1	1145.9	1228.7	1316.2	1403.0	1488.5	1574.9	1660.4	1744.5	1833.7	1920.5		

TABLE 2. The incomplete RF sequence and the calculated L.

i	1	2	3	4	5	6	7	8	-	9	10	T(℃)	L(m)
$[n(i)]$	12	13	14	15	16	17	18	9	-	21	-	27	1.89
RF (Hz)	1058.5	1145.6	1233.8	1316.6	1401.7	1492.2	1575.0	1659.8	-	1832.0	1920.2		

Note: "-" means "null".

uncertain, imprecise, and incomplete information, and what's more presents Dempster's rule to combine multiple pieces of evidence coming from different information sources. The presented fusion mechanism can effectively reduce information uncertainties and yield more accurate results than any single sensor or information source. Therefore, DST has already been widely used in pattern recognition [15]–[17], system safety assessment [18], multi-attribute decision-making [19] and so on.

Let $\Theta = \{\theta_1, \theta_2, \ldots, \theta_n, \}$ be a set of possible answers to a given question, called the frame of discernment (FoD). Its power set is denoted as 2^{Θ}.

A function $m : 2^{\Theta} \rightarrow [0, 1]$ is defined as a basic belief assignment (BBA) on Θ, if it satisfies $m(\emptyset) = 0$ and $\sum_{A\subseteq\Theta} m(A) = 1$. The BBA assigns a "mass of belief" to each subset A of Θ. A subset A with $m(A) > 0$ is called a focal element (FE) of Θ. This function is also called a body of evidence (BoE), abbreviated to evidence. If A is a singleton set $\{\theta\}$ of Θ, then m reduces to the probability measure on Θ.

If m_1, m_2 are two BBAs obtained from two independent information sources, then Dempster's rule is used to combine them to generate the fused BBA as $m = m_1 \oplus m_2$, in which the belief degree of the focal element C can be obtained by

$$m(C) = \frac{\sum_{A\cap B=C} m_1(A)m_2(B)}{1 - \sum_{A\cap B=\emptyset} m_1(A)m_2(B)} \tag{14}$$

here, $\sum_{A\cap B=\emptyset} m_1(A)m_2(B)$ is called normalization factor for measuring the degree of conflict between m_1 and m_2. It is easy to be proved that Dempster's rule satisfies the commutative law ($m_1 \oplus m_2 = m_2 \oplus m_1$) and the associative law ($(m_1 \oplus m_2) \oplus m_3 = m_1 \oplus (m_2 \oplus m_3)$) [11], hence it can realize recursive fusion of multiple BBAs. This rule is the core of DST, by such fusion process, the belief degree is focused on such focal element that m_1 and m_2 all support.

Example 1: This example is to illustrate how to combine $\text{BBA}_1(m_1)$ and $\text{BBA}_2(m_2)$ listed in Table 3 using Dempster's rule, here Θ consists of three discrete elements, namely, $\Theta = \{\theta_1, \theta_2, \theta_3\}$. Obviously, after combination, the belief degree of $\{\theta_2\}$ increases because it is supported by both of BBAs, meanwhile the belief degree of "the complete unknown Θ" remarkably decreases.

Example 2: Most researchers have focused on the case of the discrete elements, actually [20] defined the field of real number as FoD, namely $\Theta = [-\infty + \infty]$ which further extends the application of Dempster's rule. Table 4 shows how to combine two BBAs with the interval-type FEs. Different from discrete case, here the new interval FEs are generated and assigned belief degrees by the intersection operation "$\cap$" in (14). Here, the belief degree is focused on the narrower interval [1400.0, 1404.7] than any FE in BBA_1 and BBA_2. In the following section, RFs with uncertainties

TABLE 3. The combination of BBAs on the discrete element field.

BBA_1		BBA_2		$BBA_{1\oplus2}$	
FE_1	m_1	FE_2	m_2	$FE_{1\oplus2}$	$m_{1\oplus2}$
$\{\theta_1\}$	0.1	$\{\theta_1\}$	0	$\{\theta_1\}$	0.04
$\{\theta_2\}$	0.3	$\{\theta_2\}$	0.4	$\{\theta_2\}$	0.45
$\{\theta_3\}$	0.2	$\{\theta_3\}$	0.1	$\{\theta_3\}$	0.16
$\{\theta_2,\theta_3\}$	0.1	$\{\theta_2,\theta_3\}$	0.3	$\{\theta_2,\theta_3\}$	0.25
Θ	0.3	Θ	0.2	Θ	0.1

TABLE 4. The combination of BBAs on the real number field.

BBA_1		BBA_2		$BBA_{1\oplus2}$	
FE_1	m_1	FE_2	m_2	$FE_{1\oplus2}$	$m_{1\oplus2}$
[1398.7,1404.7]	0.88	[1400,1406]	0.87	[1400.0,1404.7]	0.78
				[1400.0,1406.0]	0.11
[1392.7,1410.7]	0.12	[1394,1412]	0.13	[1398.7,1404.7]	0.10
				[1394.0,1410.7]	0.01

will be modeled as the corresponding interval-type BBAs and fused.

B. THE DEFINITION OF THE RANDOM-FUZZY VARIABLES (RFV)

International Electrotechnical Commission has proposed a guide to the expression of uncertainties in measurement [21]. In this guide, when the uncertainty of data collected by information source or sensor is stemmed from random disturbance in measurement environment, the statistical approach is suggested to model this kind of random uncertainty, because the statistics concentrates on handling the statistical distributions of data. But it seems helpless for such data that are simultaneously affected by non-randomness, i.e., unknown systematic uncertainty. This kind of non-random uncertainty commonly comes from the mixture of some factors, for example in the level gauge, the systematic error of the microphone and the quantization errors of the A/D converter and the signal conditioning circuit in the controller. It is known that fuzzy variable is an available tool to model the non-random uncertainty. In a word, single statistical method or fuzzy method can hardly comprehensively deal with these two different uncertainties, but random-fuzzy variable (RFV) proposed in [22], [23] can naturally do that because it can effectively express the contributions of different effects (random and unknown systematic) to uncertainties of sensor data.

The RFV is a particular kind of a type-II fuzzy variables whose α-cut B_α is the type- II confidence interval

$$B_\alpha = \left[\left[b_1^\alpha, b_2^\alpha\right]_2 \left[b_3^\alpha, b_4^\alpha\right]\right] \quad \text{for} \quad \forall\alpha \in [0,1] \qquad (15)$$

It obeys the following constraints [21]:

1) For $\forall\alpha \in [0,1]$, $b_1^\alpha \le b_2^\alpha \le b_3^\alpha \le b_4^\alpha$;
2) When α is taken value in [0,1], B_α can be divided two type-I confidence interval sequences, namely the external sequence $ES = \{[b_1^\alpha, b_4^\alpha]|\alpha \in [0,1]\}$ and the inner sequence $IS = \{[b_2^\alpha, b_3^\alpha]|\alpha \in [0,1]\}$. Thus, ES and IS can be used to generate the normal and convex membership function (MF);
3) For $\forall\alpha, \alpha' \in [0,1]$

$$\alpha' > \alpha \Rightarrow \begin{cases} [b_1^{\alpha'}, b_3^{\alpha'}] \subset [b_1^\alpha, b_3^\alpha] \\ [b_2^{\alpha'}, b_4^{\alpha'}] \subset [b_2^\alpha, b_4^\alpha] \end{cases} ;$$

4) $[b_1^{\alpha=1}, b_2^{\alpha=1}] \equiv [b_3^{\alpha=1}, b_4^{\alpha=1}]$.

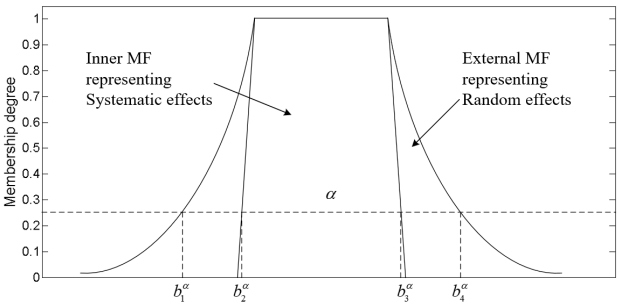

FIGURE 4. Structure of a RFV.

Fig.4 gives an example of RFV whose B_α has the confidence level $\beta = 1 - \alpha$, such as $\alpha = 0.25, \beta = 1 - 0.25 = 0.75$. Hence, an RFV can be established by combining its inner and external membership functions according to their α-cuts for all possible $\alpha \in$[0,1]. When the RFV is adopted to model uncertainties of data, the widths of the external intervals $[b_1^\alpha, b_2^\alpha]$ and $[b_3^\alpha, b_4^\alpha]$ in (15) reflect randomness contribution to whole uncertainties; the internal interval $[b_2^\alpha, b_3^\alpha]$ is a type-I confidence interval and its width reflects the contribution of the unknown systematic error to whole uncertainties.

As a result, the RFV can model not only randomness and unknown systematic error together, but also distinguish their

different contributions to whole uncertainties by using a unified form. In next section, we first use the RFVs to model the RF data collected by the level gauge in Fig.1 and then transform them to the corresponding pieces of evidence (BBAs) for combination by using Dempster's rule as shown in Example 2.

IV. THE RECURSIVE FUSION METHOD OF RF EVIDENCE SEQUENCES VIA RFV AND DST

This section will present a new level detection procedure by using the RFV-based model and the DST-based fusion mechanism introduced in Section III. It involves the following steps: (1) modeling of RFV via historical resonance frequency data; (2) acquisition of RF evidence (BBA) from the RFV models; (2) recursive fusion of the intact and incomplete RF evidence sequences; (3) level calculation according to the fused result. The aims of this proposed procedure lie in two aspects, one is to improve the frequency detection stability by supplementing the missed RF points; another is to improve the measurement accuracy even if only intact RF evidence sequences need to be fused without the missing cases.

A. CNOSTRUCT RFV MODEL OF RF BY THE HISTORICAL DATA

For a certain RF, three steps are needed to get its RFV: 1) model the external membership function μ_E for randomness contribution; 2) model the inner membership function μ_I for non-randomness contribution; 3) obtain the RFV by integrating μ_E and μ_I.

1) MODEL THE EXTERNAL FUNCTION μ_E

Suppose x is a monitored variable denoting a certain RF. Given a certain detected height L, x was observed by the level gauge in Fig.1, q sample values of x were recorded, generally $q \geq 200$. Thus, its statistical histogram can be plotted by using these historical data. The probability density function (pdf) of x is approximated through interpolation fitting with Gaussian model [23].

Example 3: For the example of $L = 2$ m in Fig.2, let $x = f(i), i = 5, n(i) = 16$. Going through q observation periods, q RF sequences can be collected, accordingly q sample values of x can be extracted, such as $x = 1403$ Hz in Table 1. Hence, the pdf $p(x)$ can be fitted from the histogram plotted based on q samples as shown in Fig.5.

The next step is to transform $p(x)$ to the corresponding μ_E. Firstly, let $x_p = \max_x(p(x))$ be the peak value or mean value of $p(x)$, its membership degree $\mu_E(x_p)$ is set to 1. Let x_L and x_R be the left and right bounds of x respectively and the corresponding interval $[x_L, x_R]$=$[x_p - 3\sigma, x_p + 3\sigma]$, σ is the standard deviation of x. Secondly, the sub-interval $[x_{Lj}, x_{Rj}]$ is extracted from $[x_L, x_R]$, $j = 1, 2, \ldots, J$, here, $x_{Lj} = x_L + j \times (x_p\text{-}x_L)/(J+1)$, $x_{Rj} = x_p + (J\text{-}j+1) \times (x_R\text{-}x_p)/(J+1)$, so x_{Lj}, x_{Rj} are located in both sides of x_p respectively in symmetry as shown in Fig.6 such that $J + 2$ nested intervals

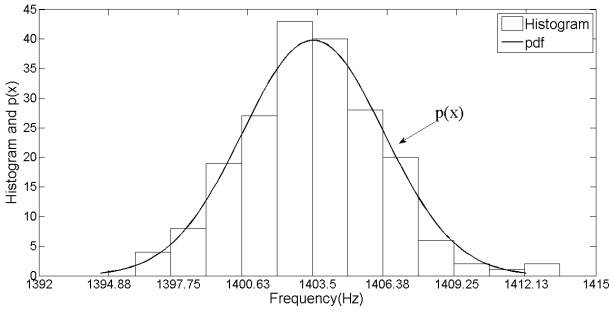

FIGURE 5. The fitted Gaussian pdf for $x = f(5)$, $L = 2$m.

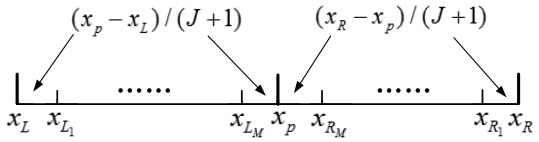

FIGURE 6. The sub-intervals and their endpoints.

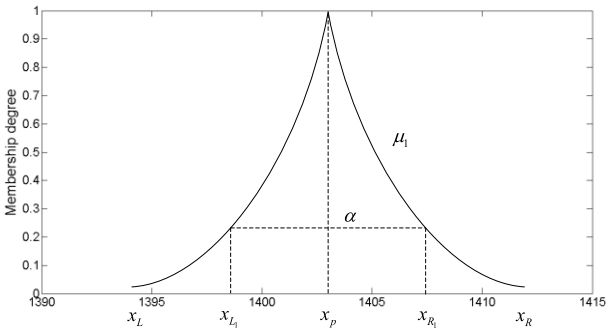

FIGURE 7. The external membership function μ_E for $x = f(5)$, $L = 2$m.

can be listed as $[x_p, x_p] \subseteq [x_{L_J}, x_{R_J}] \subseteq [x_{L_{J-1}}, x_{R_{J-1}}] \subseteq \ldots \subseteq [x_{L_1}, x_{R_1}] \subseteq [x_L, x_R]$.

Actually, these sub-intervals can be considered as the different α-cuts of the membership function μ_E. The greater J is, the higher the resolution of the desired fuzzy variable is. The value of J is determined based on actual requirement. It is known that the confidence level about the sub-interval $[x_{L_j}, x_{R_j}]$ is [21]–[23]

$$\beta_j = \int_{x_{L_j}}^{x_{R_j}} p(x)dx \tag{16}$$

thus the corresponding $\alpha_j = 1 - \beta_j$. In Example 3 for $x = f(i)$, $i = 5$, we have $J = 50$, $x_p = 1403.37$, $x_L = 1394.81$, $x_R = 1411.93$, $\sigma = 0.0061$, using $J + 2$ nested intervals (α-cuts), $p(x)$ can be transformed into μ_E as shown in Fig.7

2) MODEL THE INNER FUNCTION μ_I

μ_I is used to model the non-randomness uncertainty derived from the systematic error of sensor instruments, namely the microphone in the designed level gauge. Generally, the systematic error can be directly provided by manufacturer with the form $x_p(1 \pm \delta\%)$, here δ denotes maximal deviation for

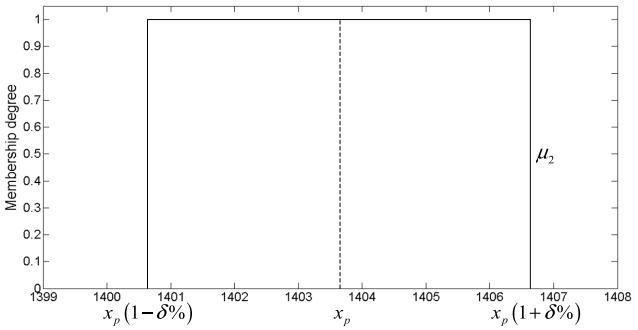

FIGURE 8. Inner rectangular membership function μ_I for $x = f(5)$, $L = 2$m.

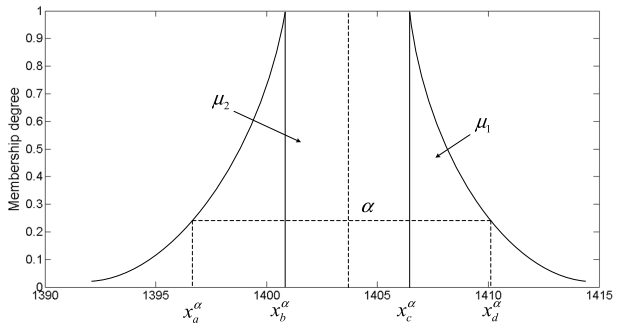

FIGURE 9. The generated RFV.

measuring sensor accuracy, for the used microphone $\delta = 0.4$. Fig.8 shows μ_I of Example 3 for $x = f(i)$, $i = 5$. Furthermore, If more data or expert advice can be obtained, the form of the membership function may be revised, no longer rectangular generally [22], [23].

3) GENERATE THE RFV BY INTEGRATING μ_E AND μ_I

After getting μ_E and μ_I, the corresponding RFV can be generated. Still using Example 3 for $x = f(i)$, $i = 5$, Fig.9 gives the corresponding RFV by integrating μ_E and μ_I. At a certain level α, the generated α-cuts of μ_E and μ_I are denoted as $[x^\alpha_{E_L}, x^\alpha_{E_R}]$ and $[x^\alpha_{I_L}, x^\alpha_{I_R}]$ respectively. $[x^\alpha_{E_L}, x^\alpha_{E_R}]$ is divided into the two intervals $[x^\alpha_{E_L}, x_p]$ and $[x_p, x^\alpha_{E_R}]$. The α-cut $X_\alpha = \{x^\alpha_a, x^\alpha_b, x^\alpha_c, x^\alpha_d\}$ of the RFV is defined by

$$\begin{aligned} x^\alpha_b &= x^\alpha_{I_L} \\ x^\alpha_c &= x^\alpha_{I_R} \\ x^\alpha_a &= x^\alpha_b - (x_p - x^\alpha_{E_L}) \\ x^\alpha_d &= x^\alpha_c + (x^\alpha_{E_R} - x_p) \end{aligned} \tag{17}$$

B. OBTAIN THE RF EVIDENCE (BBA) FROM THE HISTORICAL RFV MODELS

For an unknown detected height L, after the level gauge implements one time sound reflection process, a RF sequence can be online extracted as shown in Table 2 ($L = 2$ m). For a certain RF point $f(i)$, we can construct its BBA with the form of two interval-type focal elements (FEs) as follows

$$BBA_i = \{([l_0, r_0], m_i([l_0, r_0])), ([l_1, r_1], m_i([l_1, r_1])\} \tag{18}$$

1) SET THE FES BY THE HISTORICAL RFV MODELS

After the historical RF data are recorded, for a certain known height L and its certain RF point x, the procedure introduced in Section 4.1 can be used to construct the corresponding RFV with its α-cuts as shown in (17). Let $\alpha = 1$ and 0, we have its two special α-cuts as

$$X_{\alpha=1} = \{x^1_a, x^1_b, x^1_c, x^1_d\} \rightarrow \begin{cases} x^1_a = x^1_b = x_p(1-\delta\%) \\ x^1_c = x^1_d = x_p(1+\delta\%) \end{cases} \tag{19}$$

$$X_{\alpha=0} = \{x^0_a, x^0_b, x^0_c, x^0_d\} \rightarrow \begin{cases} x^0_b = x_p(1-\delta\%) \\ x^0_c = x_p(1+\delta\%) \\ x^0_a = x^0_b - (x_p - x^\alpha_{E_L}) \\ x^0_d = x^0_c + (x^\alpha_{E_L} - x_p) \end{cases} \tag{20}$$

From (19) and (20), we can construct two intervals $[x^1_a, x^1_d]$ and $[x^0_a, x^0_d]$ respectively and $[x^1_a, x^1_d] \subset [x^0_a, x^0_d]$. The former denotes the minimum uncertainty degree, only considering the unknown systematic error, the latter represents the maximum uncertainty degree emphasizing the mixture of random error and systematic error. It is obvious that $[x^1_a, x^1_d]$ and $[x^0_a, x^0_d]$ are symmetrical to x_p, so we define the minimum confidence factor u^1 and the maximum confidence factor u^0 respectively as

$$u^1 = x_p - x^1_a = x^1_d - x_p, u^0 = x_p - x^0_a = x^0_d - x_p, u^1 < u^0 \tag{21}$$

Suppose there have been Q historical RFV models for the different heights L and its different RF points, then the mean values of two factors can be calculated as

$$\bar{u}^1 = \sum_{q=1}^{Q} u^1_q \Big/ Q, \bar{u}^0 = \sum_{q=1}^{Q} u^0_q \Big/ Q, \bar{u}^1 < \bar{u}^0 \tag{22}$$

As a result, when a certain RF point $f(i)$ of an unknown detected height L is online obtained, its two FEs can be constructed as

$$\begin{aligned} [l_1, r_1] &= [f(i) - \bar{u}^1, f(i) + \bar{u}^1], [l_0, r_0] \\ &= [f(i) - \bar{u}^0, f(i) + \bar{u}^0], [l_1 r_1] \subset [l_0, r_0] \end{aligned} \tag{23}$$

2) SET THE BELIEF DEGREES OF THE FES BY THE AMPLITUDE OF RF POINT $F(I)$

When the RF point $f(i)$, $i = 1, 2, \ldots, M$ is online detected, at the same time its amplitude can be get and denoted as $A(i)$, we have

$$A_{\max} = \max\{A(i) | i = 1, 2, \ldots, M\} \tag{24}$$

Thus, the belief degrees of $[l_1,r_1]$ and $[l_0,r_0]$ can be defined as

$$m_i([l_1, r_1] = (A_{\max} - A(i)) \Big/ A_{\max}, m_i([l_0, r_0] = 1\text{-}m_i([l_1, r_1]) \tag{25}$$

That is to say, the RF point with large amplitude is more easily detected and more reliable than the others, and its FE $[l_1,r_1]$ with minimum uncertainty should be assigned the

larger belief degree than $[l_0,r_0]$ with maximum uncertainty, vice versa.

Example 5: Assume Table 2 lists the online detected RF sequence here we never know the value of L in advance, the corresponding amplitudes are marked in Fig.3. Obviously, $A_{\max} = A(6) = 5.5\times10^{-4}$, $A_{\min} = A(3) = 3.4\times10^{-4}$, so we have

$$\begin{aligned} m_6([l_1, r_1] &= {}^{(A_{\max} - A(6))}/_{A_{\max}} \\ &= 1, m_6([l_0, r_0] = 1 - m_6([l_1, r_1] = 0 \\ m_3([l_1, r_1] &= {}^{(A_{\max} - A(3))}/_{A_{\max}} \\ &= 0.38, m_3([l_0, r_0] = 1 - m_3([l_1, r_1] = 0.62 \end{aligned}$$

Here, the RF point with largest amplitude is regarded as a benchmark, the BBAs of other RFs can be calculated by comparing with it.

C. RECURSIVELY COMBINE THE RF EVIDENCE SEQUENCES

For an unknown detected height L, the level gauge can continuously repeats K times sound reflection processes and then K RF sequences can be extracted in which the k^{th} sequence ($k = 1, 2, \ldots, K$) is denoted as $RFS_k = \{f_k(i)|i = 1, 2, \ldots, M_k\}$. By using the method in Section 4.2, the k^{th} RF evidence sequence can be accordingly constructed as $ES_k = \{BBA_{k,i}|i = 1, 2, \ldots, M_k\}$. Thus, Dempster's rule can be used to recursively combine adjacent evidence sequences as follows

$$ES_{1:k} = ES_{1:k-1} \oplus ES_k \tag{26}$$

In order to understand (26), we illustrate how to calculate the first $ES_{1:2}$ by combining $ES_{1:1}$ and ES_2, here $ES_{1:1} = ES_1$ at the first step such that the following fusion operation can be recursively implemented in the same way. On the whole, there are three cases in the fusion operation $ES_{1:1} \oplus ES_2$.

1) CASE 1: ES_1 AND ES_2 ARE ALL INTACT EVIDENCE SEQUENCES

In this case, $M_1 = M_2$, Fig.10 shows the fusion processes for a certain $BBA_{1,i}$ in ES_1. Here, $[l_1,r_1]$ and $[l_0,r_0]$ are sketched by the narrow and wide intervals respectively. The combined $BBA_{1:2,i} = BBA_{1,i} \oplus BBA_{2,i}$ with four new interval-type FEs by using "$\cap$"operation in (14), but for the other $BBA_{2,i}(i = 1, 2, \ldots, i-1, i+1, \ldots, M_2)$, since there are the large distance between $f_1(i)$ and $f_2(i)$, the intersection of their interval FEs must be the null set as shown in Fig.10. The similar fusion process can be found in the above Example 2 of Section 3.1. When this fusion process "$\oplus$" of Dempster's rule is repeated M_1 times, $BBA_{1:2,i}$ can be obtained, finally $ES_{1:2} = \{BBA_{1:2,i}|i = 1, 2, \ldots, M_1\}$ can be got by $M_1 \times M_2$ times such fusion calculations.

On the other hand, there is a "combination explosion problem", namely if ES_3 is also intact at the 3rd time step, $BBA_{1:2,i}$ with four FEs will be combined with $BBA_{3,i}$ with two

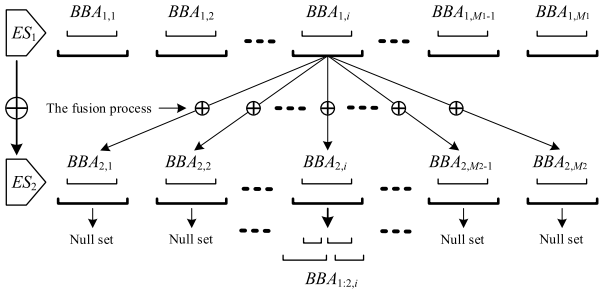

FIGURE 10. The fusion process between two intact ESs.

FEs to generate $BBA_{1:3,i}$ with eight FEs. In this way, the number of the generated FEs will increase exponentially at the following time step, it leads to unacceptable computational burden. Hence, it is necessary to simplify $BBA_{1:2,i}$. In detail, the combined $BBA_{1:2,i}$ in Fig.10 is described with the form as follows

$$BBA_{1:2,i} = \left\{([l'_t, r'_t], m_i([l'_t, r'_t]) \,|t = 0, 1, 2, 3\right\} \tag{27}$$

then the estimated resonance frequency can be calculated by

$$f'_{1:2}(i) = \sum\nolimits_{t=0}^{3} \frac{1}{2}(l'_t + r'_t)m_{1:2}([l'_t, r'_t] \tag{28}$$

namely the weighted sum of the midpoints of those four interval FEs [14]. Again using (23), we can construct two simplified EFs as

$$\begin{aligned} [l_1, r_1] &= [f'_{1:2}(i) - \bar{u}^1, f'_{1:2}(i) + \bar{u}^1], [l_0, r_0] \\ &= [f'_{1:2}(i) - \bar{u}^0, f'_{1:2}(i) + \bar{u}^0] \end{aligned} \tag{29}$$

and then calculate their belief degrees by using the normalized interval Euclidean distance between the new two FEs in (29) and the original four FEs in (27)

$$\begin{aligned} D_{s,t}\left([l_s, r_s], [l'_t, r'_t]\right) = \sqrt{\frac{1}{2}\left(\left|l_s - l'_t\right|^2 + \left|r_s - r'_t\right|^2\right)}, \\ s = 0, 1, t = 0, 1, 2, 3 \end{aligned} \tag{30}$$

here, $|\cdot|$ means the absolute value, thus we have

$$m_{1:2}([l_s, r_s] = \sum\nolimits_{t=0}^{3} \frac{D_{s,t}}{\sum_{s=0}^{1} D_{s,t}} m_i([l'_t, r'_t] \tag{31}$$

namely the weighted sum of the original four belief degrees in (27).

Actually, the simplified $BBA_{1:2,i}$ with two FEs in (29) and the corresponding belief degrees in (31) can be deemed as the approximate form of the original one in (27) [24]. In this way, in the following time step, $BBA_{1:k,i} = BBA_{1:k-1,i} \oplus BBA_{k,i}$ will always has only two EFs so as to reduce the computational burden.

2) CASE 2:ES_1 IS INCOMPLETE AND ES_2 IS INTACT

In this case, $M_1 < M_2$, Fig.11 shows the fusion processes for $BBA_{2,i}$. Here, the $BBA_{1,i}$ corresponding to $BBA_{2,i}$ is missed because $f_1(i)$ cannot be detected in the synthesis wave, thus directly let $BBA_{1:2,i} = BBA_{2,i}$ such that the missed BBA is

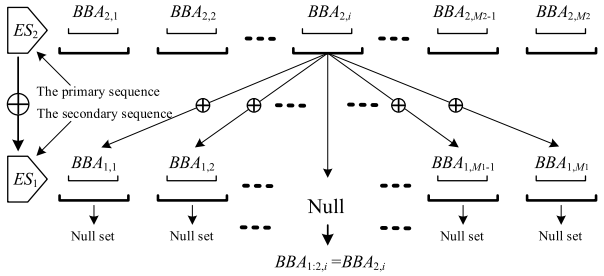

FIGURE 11. The fusion process between an intact ES and an incomplete ES.

supplemented. The similar incomplete sequence have been demonstrated by the example in Fig.3 and Table.2, Since $M_1 < M_2$, ES_2 and ES_1 are called the primary sequence and the secondary sequence respectively which means that each of *BBA* in the primary sequence must be combined with all BBAs in the secondary sequence. Certainly, in Case 1, $M_1 = M_2$, we can optionally choose one is primary, another is secondary.

As a result, after $M_1 \times M_2$ times fusion calculations, we can still get an intact evidence sequence $ES_{1:2} = \{BBA_{1:2,i} | i = 1, 2, \ldots, M_2\}$ even if ES_1 is incomplete with one or more than one missed BBAs or RFs.

3) CASE 3: ES_1 AND ES_2 IS ARE ALL INCOMPLETE EVIDENCE SEQUENCES

In level detection experiments, there are rarely two or more than two successive incomplete sequences, namely most of sequences are intact but we still discusses this case for possible requirements. Obviously, it is similar with Case 2, given M is the number of RFs in an intact RF sequence and $M_1 < M$, $M_2 < M$, if $M_1 < M_2$, then ES_2 is set as the primary sequence, ES_2 is the secondary sequence.

It should be noted that, in either case, we do not know "the intact number M" in advance, but can detect M_1 and M_2, so above three cases come down to two cases, namely, $M_1 = M_2$ and $M_1 \neq M_2$. In a word, by using recursive fusion method, as long as an intact sequence appears at a certain time step, the fused RF evidence sequences will be all intact at the following all steps.

D. CALCULATE L FROM THE FUSED RF EVIDENCE SEQUENCE

By using the procedure proposed in Section 4.3, the fused $ES_{1:k} = \{BBA_{1:k,i} | i = 1, 2, \ldots, M_{1:k}\}$ can be recursively obtained at the k^{th} time step. For each $BBA_{1:k,i}$, (28) can be used again to calculate the estimated resonance frequency as

$$f_{1:k}(i) = \sum_{s=0}^{1} \frac{1}{2}(l_s + r_s) m_{1:k}([l_s, r_s]) \tag{32}$$

and then substituting (32) into (13), the estimated level $\bar{L}$ can be got finally.

As a result, Fig.12 shows the flowchart of the recursive fusion of the RF evidence sequences to get the estimated detected height at each time step.

V. THE LEVEL DETECTION EXPERIMENTS AND PERFORMANCE CONTRASTIVE ANALYSIS

A. HARDWARE SET-UP OF THE LEVEL GAUGE

Fig.13 shows the hardware set-up designed in [10]. Here, the embedded system (STM32F746NG, STMicroelectronics, CH) is set as the controller, in which, the audio card (82801HBM-ICH8M, Intel, USA) generates the acoustic signal and commands the speaker (F10, Leadsound, CHN) to transmit the generated acoustic wave uniformly changing in the range [f_l = 1000 Hz to f_h = 2000 Hz] within 2 s. The microphone (SM012, Senic, CHN) receives the synthesis wave and sends them to the database storage units of the controller. The temperature sensor (DS18B20, Dallas semiconductor, USA) synchronously collects temperature data and sends them to the controller. The PVC tube with diameter 75 cm is used as the waveguide vertically placed in the tank containing the distilled water. The several tubes with different lengths and joints are flexibly combined to generate the different detected heights L.

The measurement range is set from 0.4 m to 10.6 m, the minimum L = 0.4 m corresponds to the minimum number of RFs (M) because (13) needs at least 2 RFs appearing in $[f_L, f_H]$ to calculate L. The experiments are conducted in the open air environment. Using this experiment set-up, as the examples, the above Figs.2∼3 and Tables.1∼2 have illustrated the extracted intact and incomplete RF sequences and the calculated L respectively.

B. CONSTRUCTION OF THE RFV MODELS OF RFS BY THE HISTORICAL DATA

According to the flowchart in Fig.12, before the proposed fusion method is put into effect, the primary mission is to construct the historical RFVs. Their minimum confidence factors u^1 and the maximum confidence factors u^0 can be obtained by (21), and then the mean values $\bar{u}^1$ and $\bar{u}^0$ of these two factors are calculated by (22) for constructing the FEs of the RF test sample by (23). Here, we set $L = 0.5, 0.7, \ldots, 10.3, 10.5$ m with 0.2 m step length. For each value of L, the level gauge in Fig.13 is used to implements 200 times sound reflection processes, thus for all 52 values of L from 0.5m to 10.5m, the total 1619 RF points can be extracted. For each RF point, there are 200 samples for constructing its external membership function μ_E by using (16). As for the inner membership function μ_I, the accuracy of the used microphone is $\delta = 0.4$ when the received frequencies are in [1000Hz, 2000Hz], then for 1619 RFs, they have the same μ_I as shown in Fig.8. Consequentially, the RFVs of 1619 RFs can be constructed by using the method in Section 4.1 and the mean values of u^1 and u^0 can be obtained as $\bar{u}^1 = 3.01$Hz and $\bar{u}^0 = 8.99$Hz.

C. THE COMPARATIVE EXPERIMENTS

In this section, two typical experiments are given to compare the proposed recursive evidence fusion method (REF method for short) with the single RF sequence-based detection method without considering the missing of

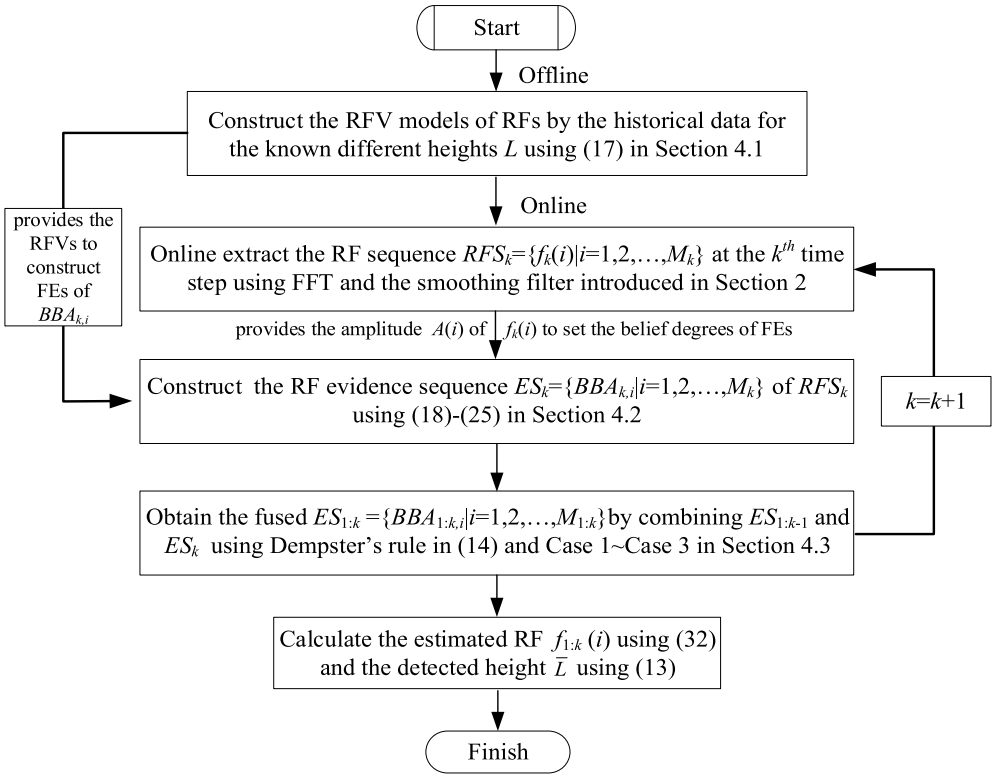

FIGURE 12. The flowchart of the recursive fusion of the RF evidence sequences.

FIGURE 13. Hardware set-up of the level gauge.

RF (SIN method) and the limit range filter for solving the missing problem of RF points (LRF method). Experiment 1 presents the detailed calculation process of the proposed method for L =2m, Experiment 2 makes performance statistical analysis for the different testing heights from 0.4 m to 10.6 m.

Before these experiments, we firstly introduce the LRF method. From (4) and (6), it can be deduced

$$L=\frac{n(i)c}{2f(i)}=\frac{n(i+1)c}{2f(i+1)}=\frac{c}{2f_1} \tag{33}$$

here f_1 is the fundamental RF as shown in (5), thus

$$n(i)f_1=f(i),\ n(i+1)f_1=f(i+1) \tag{34}$$

$$f(i+1)-f(i)=n(i+1)f_1-n(i)f_1=f_1 \tag{35}$$

That is to say, theoretically the difference between $f(i+1)$ and $f(i)$ is equal to the fundamental RF (f_1) as shown in Fig. 2(b) and Table 1 for L = 2 m, here RF points appear at regular interval (f_1) in intact case. But in the missing case as shown in Fig.3(b) and Table 2, when i = 9, the RF point is missed, so $f(i+1)$-$f(i)$ > f_1. Here, the mean value of the interval is calculated as

$$\bar{f}_1=\sum_{i=1}^{M-1}(f(i+1)-f(i))=\sum_{i=1}^{M-1}f_1^i \tag{36}$$

which can be considered as an indicator or a threshold value for identifying two cases. In detail, when $(f(i+1)-f(i))>f_1>\bar{f}_1$, there could be one or more the missed RF points between $f(i+1)$ and $f(i)$, otherwise there could be not the missed points, $f(i+1)-f(i)\approx f_1$, because in practice, the uncertain disturbances in measurement environment will cause $(f(i+1)-f(i))$ is only the approximate value of f_1. As a result, the limit range filter can be constructed as [26]

$$f_1^i=\begin{cases}f_1^{i-1}, & (f(i+1)-f(i))>\bar{f_1}\\ f(i+1)-f(i), & \text{otherwise}\end{cases} \tag{37}$$

thus, the detected height can be calculated as

$$L^{LRF}=\sum_{i=1}^{M'-1}\frac{c}{2f_1^i} \tag{38}$$

which is the mean value of $M\prime$ times calculations using the approximate value of f_1 by (33). Here, $M\prime \le M$ because when

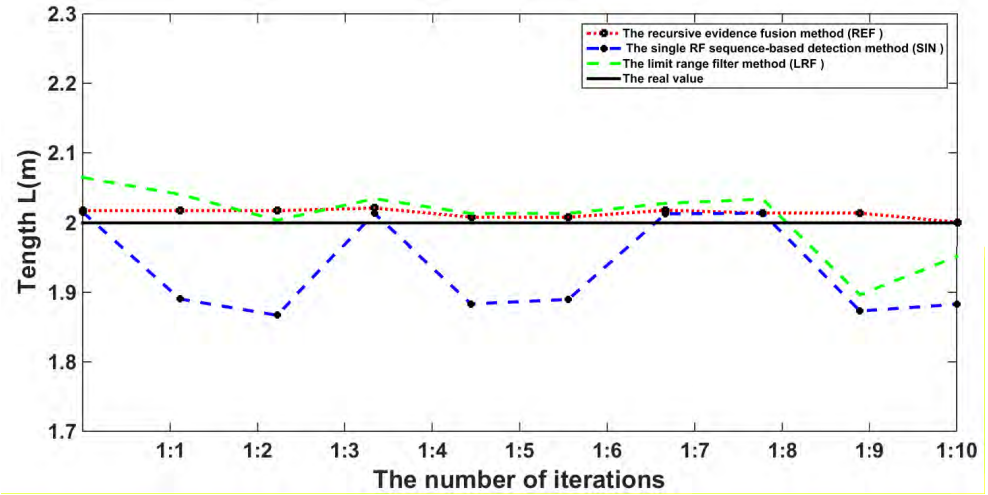

FIGURE 14. The comparative analysis of the different methods ($L = 2$m).

TABLE 5. The RF sequences collected at the successive 10 measurement periods ($L = 2$ m).

k	1	2	3	4	5	6	7	8	9	10	11
1	1059.18	1145.65	1230.10	1321.96	1403.72	1496.58	1579.69	1665.82	1751.95	1835.73	1925.91
2	1059.52	1146.32	1233.80	1319.60	1405.06	1496.58	1579.69	**null**	1751.95	1840.44	1924.90
3	1059.18	1145.65	1232.79	1319.94	1404.39	1497.25	**null**	1661.11	1752.63	1836.41	1926.58
4	1059.52	1145.65	1231.45	1320.27	1404.05	1491.20	1581.71	1663.80	1752.63	1836.74	1925.91
5	1059.52	1145.65	1231.11	1320.27	1404.05	1490.86	1581.71	**null**	1752.96	1836.74	1925.91
6	1059.52	1147.00	1234.48	1320.27	1409.77	1496.58	1580.02	**null**	1752.63	1836.41	1925.91
7	1059.18	1145.65	1232.79	1319.60	1405.40	1491.53	1581.71	1663.80	1752.63	1837.42	1925.91
8	1059.52	1145.65	1231.45	1319.94	1405.40	1490.52	1581.71	1666.83	1752.63	1836.41	1925.57
9	1059.18	**null**	1232.79	**null**	1407.08	1492.21	1581.37	1665.82	1754.98	1840.44	1925.91
10	1059.18	1145.31	1232.79	1319.94	1404.05	1497.25	1581.71	**null**	1751.95	1841.12	1925.23

TABLE 6. The level detection results of the REF, SIN and LRF methods.

1:k	1:1	1:2	1:3	1:4	1:5	1:6	1:7	1:8	1:9	1:10
$L_{1:k}^{REF}$	2.0155	2.0175	2.0175	2.0214	2.0082	2.0082	2.0182	2.0141	2.0131	2.0008
$L_{1:k}^{SIN}$	2.0155	1.8904	1.8670	2.0137	1.8834	1.8898	2.0131	2.0139	1.8731	1.8828
$L_{1:k}^{LRF}$	2.0653	2.0411	2.0039	2.0349	2.0134	2.0137	2.0281	2.0342	2.0226	2.0115

Note: "REF" means "the recursive fusion-based detection", "SIN" means "the single RF sequence-based detection", "LRF" means "the limit range filter-based detection".

there are two or more the missed RF points, (37) can only supplement one approximated fundamental RF.

Experiment 1: In order to further verify the effect of the proposed REF method, we still choose $L = 2$ m to generate the test samples as listed in Table 5 for comparing it with the SIN method and the LRF method. Table 5 lists the resonance frequency sequences $RFS_k = \{f_k(i)|i = 1, 2, \ldots, M_k\}, k = 1, 2, \ldots, 10$ collected at the successive 10 measurement periods, in which the 2^{nd}, 3^{rd}, 5^{th}, 6^{th}, 9^{th}, 10^{th} RFSs are all incomplete, specially the RFS_9 misses two RF points.

Table 6 shows the level detection results of the REF, SIN and LRF methods respectively. Here, $L_{1:k}^{SIN}$ and $L_{1:k}^{LRF}$ are obtained by the recursively weighted fusion mechanism as follows

$$L_{1:k}^{SIN} = \frac{L_{1:k-1}^{SIN} + L_k^{SIN}}{2}, L_{1:k}^{LRF} = \frac{L_{1:k-1}^{LRF} + L_k^{LRF}}{2} \quad (39)$$

Here, L_k^{SIN} and L_k^{LRF} are calculated by (13) and (38) respectively. This mechanism can reduce measurement errors to a certain degree. However, by comparative analysis of the

TABLE 7. The supplemented RF points (boldfaced format) in the incomplete sequences ($L = 2$ m).

1:k	1	2	3	4	5	6	7	8	9	10	11	$L_{1:k}^{REF}$
1:1	1059.18	1145.65	1230.10	1321.96	1403.72	1496.58	1579.69	1665.82	1751.95	1835.73	1925.91	2.0155
1:2	1059.40	1146.12	1232.66	1320.36	1404.31	1496.58	1579.69	**1665.82**	1751.95	1838.56	1925.37	**2.0175**
1:3	1059.18	1145.70	1232.77	1320.08	1404.35	1496.98	**1579.69**	1663.99	1752.48	1837.04	1926.12	**2.0175**
1:4	1059.52	1145.66	1231.73	1320.18	1404.21	1493.74	1580.80	1663.89	1752.56	1836.82	1925.99	2.0214
1:5	1059.52	1145.65	1231.23	1320.23	1404.12	1491.91	1581.30	**1663.89**	1752.77	1836.76	1925.93	**2.0082**
1:6	1059.52	1146.96	1234.00	1320.27	1406.63	1494.71	1580.62	**1663.89**	1752.66	1836.47	1925.91	**2.0082**
1:7	1059.20	1145.70	1232.90	1319.76	1405.88	1492.74	1581.17	1663.85	1752.64	1837.21	1925.91	2.0182
1:8	1059.52	1145.66	1231.57	1319.88	1405.65	1491.50	1581.46	1665.47	1752.63	1836.64	1925.62	2.0141
1:9	1059.22	**1145.66**	1232.43	**1319.88**	1406.42	1492.01	1581.41	1665.66	1754.06	1839.54	1925.88	**2.0131**
1:10	1059.19	1145.36	1232.68	1319.92	1405.11	1495.56	1581.55	**1665.66**	1752.62	1840.79	1925.30	**2.0008**

TABLE 8. One time iteration from the 8th step to the 9th step.

No	1	2	3	4	5	6	7	8	9	10	11	L
1:8	1059.52	1145.66	1231.57	**1319.88**	1405.65	1491.50	1581.46	1665.47	1752.63	**1836.65**	1925.62	2.0141
9	1059.18	**null**	1232.79	**null**	1407.08	1492.21	1581.37	1665.82	1754.98	**1840.44**	1925.91	1.8731
1:9	1059.22	1145.66	1232.43	**1319.88**	1406.42	1492.01	1581.41	1665.66	1754.06	**1839.54**	1925.88	2.0131

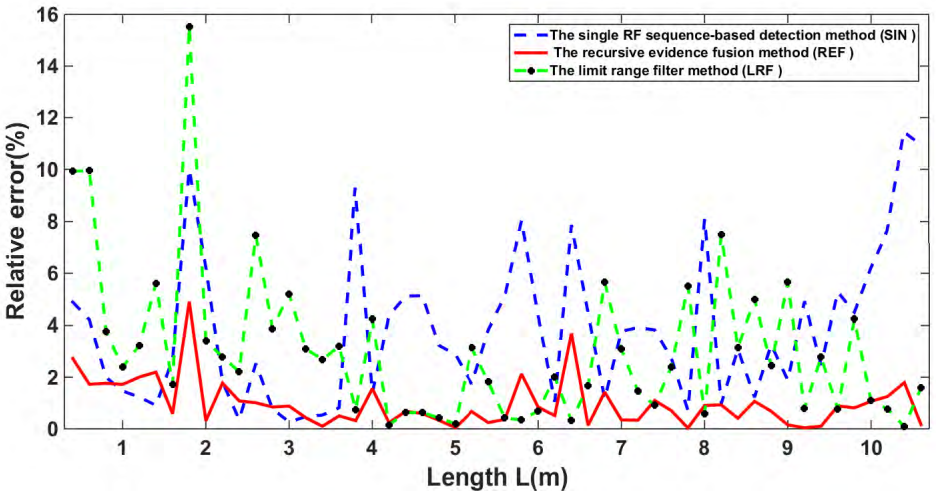

FIGURE 15. Fig.15 The relative errors for 52 testing heights from 0.4m to 10.6m.

recursive fusion results as shown in Fig.14 corresponding to Table 6, it can be seen that the estimated values of the REF method converge to the truth (L =2m) more precisely than the SIN and LRF methods.

Furthermore, Table 7 shows the supplemented RF points with boldfaced format in the incomplete sequences according to the proposed three cases in Section 4.3. Obviously, by using "$\cap$" operation in Dempster's rule, the REF method can find out the incomplete RFs and supplement the missed points, the corresponding RF evidence, even if the missing cases happen continually.

As an example, one time iteration from the 8th step to 9th step is illustrated to interpret the recursive fusion process of the REF method. Table 8 shows $ES_{1:8} = \{BBA_{8,i}|i = 1, \ldots, M_{1:8}, M_{1:8} = 11\}$, $ES_9 = \{BBA_{9,i}|i = 1, \ldots, M_9, M_9 = 9\}$ and $ES_{1:9} = \{BBA_{9,i}|i = 1, \ldots, M_{1:9}, M_{1:9} = 11\}$ respectively. When $i = 2$ (the missing case), the "$\cap$" operations between $BBA_{1:8,2}$ and $BBA_{9,i}$ generate nothing but the null sets, we judge $f_9(2)$ is missed (corresponding to Case 2 in Section 4.3), thus let $BBA_{1:9,2} = BBA_{1:8,2}$, $f_9(2)$ is calculated by (32). In the same way, $BBA_{1:9,4}$ and $f_9(4)$ can be also

TABLE 9. The comprehensive tests for 52 heights from 0.4m to 10.6m.

No	L(m)	T(℃)	$L_{1:k}^{REF}$	$L_{1:k}^{SIN}$	$L_{1:k}^{LRF}$	ε_{REF}	ε_{SIN}	ε_{LRF}
1	0.4	33	**0.4109**	0.4195	0.4397	**0.0273**	0.0489	0.0992
2	0.6	33	**0.6103**	0.6252	0.6597	**0.0172**	0.0420	0.0996
3	0.8	29	**0.8141**	0.8160	0.8301	**0.0176**	0.0200	0.0377
4	1	29	**1.0172**	1.0147	1.0240	**0.0172**	0.0147	0.0240
5	1.2	29	**1.2241**	1.2147	1.2388	**0.0200**	0.0123	0.0323
6	1.4	29	**1.4307**	1.4128	1.4784	**0.0220**	0.0091	0.0560
7	1.6	28	**1.6093**	1.5569	1.6274	**0.0058**	0.0270	0.0171
8	1.8	27	**1.8883**	1.9801	2.0795	**0.0490**	0.1000	0.1553
9	2	27	**1.9938**	1.8758	2.0682	**0.0031**	0.0621	0.0341
10	2.2	27	**2.2390**	2.1602	2.2613	**0.0177**	0.0181	0.0279
11	2.4	27	**2.4259**	2.3915	2.4531	**0.0108**	0.0036	0.0221
12	2.6	27	**2.6262**	2.6657	2.7943	**0.0101**	0.0253	0.0747
13	2.8	27	**2.8237**	2.8217	2.9085	**0.0085**	0.0078	0.0387
14	3	27	**3.0264**	3.0079	3.1558	**0.0088**	0.0026	0.0519
15	3.2	27	**3.2138**	3.2152	3.2992	**0.0043**	0.0047	0.0310
16	3.4	26.5	**3.4034**	3.4181	3.4912	**0.0010**	0.0053	0.0268
17	3.6	26.5	**3.6181**	3.6293	3.7151	**0.0050**	0.0081	0.0320
18	3.8	26.5	**3.8120**	3.4471	3.8281	**0.0032**	0.0929	0.0074
19	4	26.5	**4.0623**	3.9445	4.1688	**0.0156**	0.0139	0.0422
20	4.2	26.5	**4.1901**	4.0169	4.2063	**0.0023**	0.0436	0.0015
21	4.4	26.5	**4.4299**	4.1748	4.4275	**0.0068**	0.0512	0.0063
22	4.6	26.5	**4.6273**	4.3641	4.6292	**0.0059**	0.0513	0.0064
23	4.8	26.5	**4.8158**	4.6448	4.8201	**0.0033**	0.0323	0.0042
24	5	26.5	**4.9977**	4.8561	5.0095	**0.0005**	0.0288	0.0019
25	5.2	26.5	**5.2349**	5.1099	5.3633	**0.0067**	0.0173	0.0314
26	5.4	26.5	**5.4131**	5.1934	5.4983	**0.0024**	0.0383	0.0182
27	5.6	26.5	**5.6204**	5.3130	5.6234	**0.0036**	0.0512	0.0042
28	5.8	26.5	**5.6768**	5.3334	5.8201	**0.0212**	0.0805	0.0035
29	6	26.5	**6.0505**	5.7388	6.0414	**0.0084**	0.0435	0.0069
30	6.2	26.5	**6.2318**	6.1352	6.3243	**0.0051**	0.0105	0.0201
31	6.4	26.5	**6.1631**	5.8965	6.4203	**0.0370**	0.0787	0.0032
32	6.6	26.5	**6.5910**	6.3055	6.7099	**0.0014**	0.0446	0.0167
33	6.8	26.5	**6.8967**	6.7207	7.1841	**0.0142**	0.0117	0.0565
34	7	26.5	**6.9758**	6.7358	7.2160	**0.0035**	0.0377	0.0309
35	7.2	26	**7.1759**	6.9178	7.3047	**0.0033**	0.0392	0.0145
36	7.4	26	**7.4814**	7.1166	7.4673	**0.0110**	0.0383	0.0091
37	7.6	26	**7.6536**	7.3918	7.7824	**0.0071**	0.0274	0.0240
38	7.8	26	**7.8026**	7.7447	8.2294	**0.0003**	0.0071	0.0551
39	8	26	**7.9277**	7.3521	8.0472	**0.0090**	0.0810	0.0059
40	8.2	26	**8.2762**	8.1203	8.8137	**0.0093**	0.0097	0.0748
41	8.4	26	**8.4345**	8.1408	8.6640	**0.0041**	0.0309	0.0314
42	8.6	26	**8.6918**	8.4947	9.0297	**0.0107**	0.0122	0.0500
43	8.8	26	**8.8600**	8.5131	9.0160	**0.0068**	0.0326	0.0245
44	9	26	**9.0136**	8.8304	9.5095	**0.0015**	0.0188	0.0566
45	9.2	26	**9.2036**	8.7476	9.2717	**0.0004**	0.0492	0.0078
46	9.4	26	**9.4095**	9.1679	9.6609	**0.0010**	0.0247	0.0278
47	9.6	26	**9.5148**	9.0938	9.6743	**0.0089**	0.0527	0.0077
48	9.8	26	**9.8795**	9.3597	10.2145	**0.0081**	0.0449	0.0423
49	10	26	**9.8932**	9.3772	10.1096	**0.0107**	0.0623	0.0110
50	10.2	26	**10.0722**	9.4203	10.1224	**0.0125**	0.0764	0.0076
51	10.4	26	**10.2137**	9.2089	10.3912	**0.0179**	0.1145	0.0008
52	10.6	26	**10.5827**	9.4376	10.4323	**0.0016**	0.1097	0.0158

supplemented. When $i = 10$ (the intact case), $BBA_{1:8,10} = \{([1833.65, 1839.65], 0.67), ([1827.65, 1845.65], 0.33)\}$ has been got using (29) and (31) at the last step, $BBA_{9,10} = \{([1836.54, 1842.54], 0.76), ([1830.54, 1848.54], 0.24)\}$ calculated from $f_9(10)$ using (23) and (25). Thus, Dempster's rule in (14) can be used to calculate $BBA_{1:9,10} = BBA_{1:8,10} \oplus BBA_{9,10} = \{([1837.44, 1839.65], 0.5628), ([1833.65, 1839.65], 0.1072), ([1837.44, 1843.44], 0.2772), ([1831.44, 1845.65], 0.0528)$. Finally, the approximated $BBA_{1:9,10}$ can be obtained by (29) and (31) as $\{([1836.54,1842.54],0.76), ([1830.54, 1848.54], 0.24)\}$, $f_9(10) = 1839.54$.

Experiment 2: Total 52 testing heights from 0.4 m to 10.6 m with 0.2 m step length are taken to do the comprehensive tests for the REF method.

Each of tests includes the successive 10 measurement periods similar with Table 5. Table 9 gives the testing results, in which L is the true height, ε_{REF},ε_{SIN} and ε_{LRF} denote the relative errors of $L_{1:k}^{REF}$, $L_{1:k}^{SIN}$ and $L_{1:k}^{LRF}$ respectively. Here, most of tests all include incomplete RF sequences, except those for 0.4m ∼1.4m, 2.6m ∼2.8m,3.2m ∼3.6m.

Furthermore, Fig.15 shows relative errors for 52 testing heights from which the mean values of ε_{REF} and ε_{SIN} and ε_{LRF} can be obtained as 0.982%, 3.79% and

3.05% respectively. It is concluded that whatever the intact case or the incomplete case, most of 52 tests show the proposed REF method provides more accurate estimated results than the SIN method and the LRF method.

All in all, the SIN method completely ignores the missed RF points, the LRF method only supplements one fundamental RF in the missed interval, so both of them hardly provide the desired estimated results. On the other hand, although these three methods all use recursive fusion mechanisms, the recursive evidence fusion in the proposed REF method is obviously better than the recursively weighted fusion in the SIN and LRF methods because the former can not only precisely supplement the miss RF points, but also reduce the measurement error by using the fine RFV models and Dempster's combination rule.

VI. CONCLUSION

The evidence-based recursive fusion method is presented to improve the performance of the acoustic resonance level detector. The main contributions include: (1) The random fuzzy variable is introduced to model the uncertainties of the observed RF points; (2) by using "$\cap$" operation between interval-type focal elements constructed by the RFV model, the missed RF points can be detected and supplemented; (3) the recursive fusion of RF evidence sequences can observably increase the stability and accuracy of the level detector. Certainly, the proposed method also inherits good properties of the original detector including high insensitivity to parasitic reflections, simple and inexpensive hardware realization, etc. At the same time, it is worth noting that, the proposed method can be further united with the error compensators in [12] and [25] to further improve the measurement accuracy because the latter are fit for the intact RF sequences.

REFERENCES

[1] L. Wang, Z.-J. Zhou, C.-H. Hu, and T.-Y. Liu, "Ultrasonic testing defect recognition based on belief-rule-base and evidential reasoning," *China Meas. Test*, vol. 43, no. 4, pp. 62–67, 2017.

[2] M. A. Jacobs, R. Breeuwer, M. F. Kemmere, and J. T. F. Keurentjes, "Contactless liquid detection in a partly filled tube by resonance," *J. Sound Vibrat.*, vol. 285, nos. 4–5, pp. 1039–1048, 2005.

[3] A. Agrawal, S. C. Kor, U. Nandy, A. R. Choudhary, and V. R. Tripathi, "Real-time blast furnace hearth liquid level monitoring system," *Ironmaking Steelmaking*, vol. 43, no. 7, pp. 550–558, 2016.

[4] J.-N. Yuan, "Liquid level measurement and infusion alarm device based on infrared sensor device," *Mod. Electron. Technique*, no. 13, p. 39, 2011.

[5] D. Donlagic, M. Zavrsnik, and I. Sirotic, "The use of one-dimensional acoustical gas resonator for fluid level measurements," *IEEE Trans. Instrum. Meas.*, vol. 49, no. 5, pp. 1095–1100, Oct. 2000.

[6] D. Đonlagić, M. Završnik, and D. Đonlagić, "Low-frequency acoustic resonance level detector with neural-network classification," *Sens. Actuators A, Phys.*, vol. 55, no. 3, pp. 209–215, 1996.

[7] D. Donlagić, "A robust miniature acoustical liquid level gauge with micrometer resolution," *Rev. Sci. Instrum.*, vol. 73, no. 2, pp. 464–467, 2002.

[8] H.-C. Wang, "An automatic online pressure-type detection system for open channel flow," Ph.D. dissertation, School Hydraulic Sci. Eng., Taiyuan Univ. Technol., Taiyuan, China, 2015.

[9] M. Deghat and P. Karimaghaee, "A level measurement method based on acoustic resonance using unscented Kalman filter," *IFAC Proc. Volumes*, vol. 41, no. 2, pp. 1426–1431, 2008.

[10] X. Xu, Z. Li, G. Li, J. Li, and C. Wen, "An acoustic resonance-based liquid level detector with error compensation," *IEEE Trans. Instrum. Meas.*, vol. 68, no. 4, pp. 963–971, Apr. 2019.

[11] G. Shafer, *A Mathematical Theory of Evidence*, vol. 42. Princeton, NJ, USA: Princeton Univ. Press, 1976.

[12] X.-B. Xu, C.-P. Zhao, and B.-D. Xia, "A fluid level measurement method based on acoustical resonance in a special frequency range," *Acta Metrol. Sinica*, vol. 32, no. 1, pp. 53–57, 2011.

[13] H. Lü, W.-B. Shangguan, and D. Yu, "An imprecise probability approach for squeal instability analysis based on evidence theory," *J. Sound Vibrat.*, vol. 387, pp. 96–113, Jan. 2017.

[14] X. B. Xu, C. L. Wen, X. Y. Sun, and Y. D. Ji, *Evidence Fusion and Decision-Making Methods for Equipment Fault Diagnosis*. Beijing, China: China Science Press, 2017.

[15] Z. Liu, Q. Pan, J. Dezert, J.-W. Han, and Y. He, "Classifier fusion with contextual reliability evaluation," *IEEE Trans. Cybern.*, vol. 48, no. 5, pp. 1605–1618, May 2018.

[16] X. Xu, J. Zheng, J. Yang, D. Xu, and Y. Chen, "Data classification using evidence reasoning rule," *Knowl.-Based Syst.*, vol. 116, pp. 144–151, Jan. 2017.

[17] Z. Liu, Q. Pan, J. Dezert, and G. Mercier, "Hybrid classification system for uncertain data," *IEEE Trans. Syst., Man, Cybern., Syst.*, vol. 47, no. 10, pp. 2783–2790, Oct. 2017.

[18] X. Xu, S. Li, X. Song, C. Wen, and D. Xu, "The optimal design of industrial alarm systems based on evidence theory," *Control Eng. Pract.*, vol. 46, pp. 142–156, Jan. 2016.

[19] M. Zhou, X.-B. Liu, J.-B. Yang, Y.-W. Chen, and J. Wu, "Evidential reasoning approach with multiple kinds of attributes and entropy-based weight assignment," *Knowl.-Based Syst.*, vol. 163, pp. 358–375, Jan. 2018.

[20] P. Smets, "Belief functions on real numbers," *Int. J. Approx. Reasoning*, vol. 40, no. 3, pp. 181–223, 2005.

[21] A. Ferrero and S. Salicone, "The random-fuzzy variables: A new approach to the expression of uncertainty in measurement," *IEEE Trans. Instrum. Meas.*, vol. 53, no. 5, pp. 1370–1377, Oct. 2004.

[22] A. Ferrero and S. Salicone, "A comparative analysis of the statistical and random-fuzzy approaches in the expression of uncertainty in measurement," *IEEE Trans. Instrum. Meas.*, vol. 54, no. 4, pp. 1475–1481, Aug. 2005.

[23] A. Ferrero, M. Prioli, and S. Salicone, "Conditional random-fuzzy variables representing measurement results," *IEEE Trans. Instrum. Meas.*, vol. 64, no. 5, pp. 1170–1178, May 2015.

[24] S. Destercke, D. Dubois, and E. Chojnacki, "A consonant approximation of the product of independent consonant random sets," *Int. J. Uncertainty, Fuzziness Knowl.-Based Syst.*, vol. 17, no. 6, pp. 773–792, 2009.

[25] X. Xu, Z. Li, G. Li, and Z. Zhou, "State estimation using dependent evidence fusion: Application to acoustic resonance-based liquid level measurement," *Sensors*, vol. 17, no. 4, p. 924, 2017.

[26] S. Y. Liu, *Computer-Control System*. Beijing, China: China Machine Press, 2018.

XIAOBIN XU is a Professor with the Department of Automation, Hangzhou Dianzi University, where he is also with the Belt and Road Information Technology Research Institute. His research interests include fuzzy set theory, evidence theory and its applications in the processing of uncertain information, the reliability analysis, safety evaluation, and the condition monitoring of complex industrial systems.

DANFENG FANG is currently pursuing the degree with the Department of Automation, Hangzhou Dianzi University. His research interests include intelligent information processing, evidence theory, and its applications in acoustic signal processing.

GUO LI is currently pursuing the degree with the Department of Automation, Hangzhou Dianzi University. His research interests include intelligent information processing, evidence theory, and its applications in information fusion.

XIAOJIAN XU received the B.S. degree in energy and power engineering and the M.S. and Ph.D. degrees in marine engineering from the Wuhan University of Technology, in 2014 and 2018, respectively. She is currently a Lecturer with the School of Automation, Hangzhou Dianzi University. Her research interests include condition monitoring, the fault diagnosis of diesel engines, information fusion, and intelligent decision making.

PENG CHEN is currently pursuing the degree with Hangzhou Dianzi University. His research interests include Dempster–Shafer evidence theory and uncertain information processing.

JIANNING LI received the Ph.D. degree in control science and engineering from Zhejiang University, in 2013. He then joined the Institute of Systems Science and Control Engineering, Hangzhou Dianzi University. In 2012, he was a Visiting Student with the Department of Mechanical, Dalhousie University. His research interests include robust control, neural networks, networked control systems, and fault-tolerant control.